2020-01-1629 Published 05 Oct 2020

SAE INTERNATIONAL

Effect of Wear on Frictionally Excited Thermoelastic Instability

Yijun Qiao and Yun-Bo Yi University of Denver

Citation: Qiao, Y. and Yi, Y.-B., "Effect of Wear on Frictionally Excited Thermoelastic Instability," SAE Technical Paper 2020-01-1629, 2020, doi:10.4271/2020-01-1629.

Abstract

The effect of wear on Thermoelastic Instability (TEI) is investigated using a finite element approach. The equations of thermoelasticity, the classical wear law and the conforming contact conditions are considered. The method is based on a two-dimensional, frictional sliding model with a bimaterial interface and a simplified geometry of finite thickness. An assumption of the solution in the perturbation form leads to a quadratic eigenvalue problem. The existing analytical solutions using two infinite half planes are employed to validate the numerical solutions for several representative scenarios, including a limiting case in the absence of wear. The analytical solutions are also sought for the special cases when one of the materials is a non-conductor and when the two materials are identical, for the purpose of comparison. In general, the satisfactory agreements between the numerical and analytical approaches have been obtained. However, there are noticeable discrepancies when the wear rates of the two materials are sufficiently close to each other and when the wear rates are much greater than the critical rate. It is confirmed that wear may suppress or amplify the effect of TEI. This is consistent with the recent research findings on the same topic via an analytical approach.

Introduction

Thermoelastic instability (TEI) is a theory that explains the localized high temperatures, or hot spots on the sliding surfaces of friction components. The theory was first proposed by Barber [1] decades ago. Burton et al. applied the perturbation method to hypothesize the cause of the inhomogeneous pressure distribution and introduced the concept of a critical sliding speed for instability [2]. Most of the later researches in this area improved the theory and focused on the prediction of critical speed of TEI as well as the distribution of hot spots for clutches and brakes. For example, Dow and Burton analytically investigated TEI of sliding contact for the case of a blade sliding on a thermally conductive semi-infinite body both ignoring and considering wear. The trend of pressure variation with different material properties was studied [3]. In some cases, the presence of wear was found to give rise to oscillatory behavior where portions of the rubbing surfaces alternately rose and dropped in temperature [4]. Papangelo and Ciavarella indicated a limit value of wear coefficient above which TEI is completely suppressed [5]. They also found that the dependence of the critical speed on the material parameters is quite complex and in certain cases wear may also destabilize the system [6]. Ciavarella et al. studied TEI between two elastically similar half-planes, one of which has a sinusoidally wavy surface [7], and considered disks of finite thicknesses [8]. Lee and Barber extended the geometry to the case of a finite thickness layer sliding between two half-planes and evaluated the influence of finite disk thickness on TEI [9]. Hartsock and Fash further modified the elastic modulus of the pad in the half plane model and investigated the effect of the pad stiffness and its support structure on TEI [10]. Abbasi et al. studied the frictional heating and TEI in railway brakes considering the effect of temperature on material properties and on material wear [11]. Wang et al. established a three-dimensional transient thermo-mechanical coupling model for investigation of the distributions and coupling relationships of the temperature, stress, and displacement generated by the combination of the thermal and mechanical loads of hydro-viscous drive [12].

In addition to analytical approaches, numerical methods were also extensively used to investigate TEI by many researchers. For example, Chen studied the coupling between thermal buckling and thermoelastic instability in clutch disks using Hotspotter and ABAQUS [13]. Yi used the finite element method and higher-order eigenvalue scheme to solve the problem related to thermoelastodynamic instability (TEDI) in frictional sliding systems [14]. His group also developed a finite element model for TEI in intermittent sliding contact with realistic geometries and friction material properties [15]. Liu et al. derived an eigenfunction solution for the contact pressure variation due to wear by the finite element method [16]. Belhocine and Abdullah developed a thermomechanical model for the analysis of disc brake using a finite element commercial code [17]. Zhao et al. constructed both analytical and numerical models to study TEI in a wet clutch subjected to the mixed lubrication stage [18], then investigated the stability boundaries of thermal buckling in automotive clutches [19]. Graf and Ostermeyer provided a three-dimensional model that directly satisfied the field equations and relevant boundary conditions to estimate the critical speed and thermal mode of TEI in brakes [20]. Abdullah et al. studied the transient thermoelastic processes of multidisc dry clutch using a finite element technique, and investigated the effect of the sliding speed on the contact pressure distribution, the temperature field and the frictional heat generated along the frictional interfaces [21].

In general, the finite element method is a more convenient method to deal with complex geometries, boundary conditions and loadings compared to the analytical approach, it is therefore a preferable tool in industry. Although extensive research has been conducted on the aforementioned problems, the effect of wear on TEI has not yet been attempted using the finite element method. In this study we will follow an approach similar to the classical eigenvalue formulation for TEI problems, with the addition of the Archard wear law.

Method

1. Analytical Method

1.1 Overview of the Analytical Model The analytical model for the effect of wear developed by Papangelo and Ciavarella involves two half planes sliding at a constant velocity V [6]. Although the perturbation generally migrates in both bodies, the problem can be formulated by choosing a frame of reference (x, y, z) fixed to the perturbation and the two bodies move at speeds c_1 and c_2, respectively (see Fig. 1). The relative sliding speed, V is related to the two absolute speeds via $V = |c_1 - c_2|$. The corresponding temperature field solution, T must satisfy the thermal diffusion equation with appropriate convective terms. In Fig. 1, the out-of-plane direction is designated as y, and the in-plane directions are (x_j, z_j) with j indicating body j (j=1, 2).

With these assumptions the heat conduction equation can then be written

$$\frac{\partial^2 T_j}{\partial x^2} + \frac{\partial^2 T_j}{\partial z_j^2} + \frac{c_j}{k_j}\frac{\partial T_j}{\partial x} = \frac{1}{k_j}\frac{\partial T_j}{\partial t} \tag{1}$$

FIGURE 1 Two sliding half-spaces.

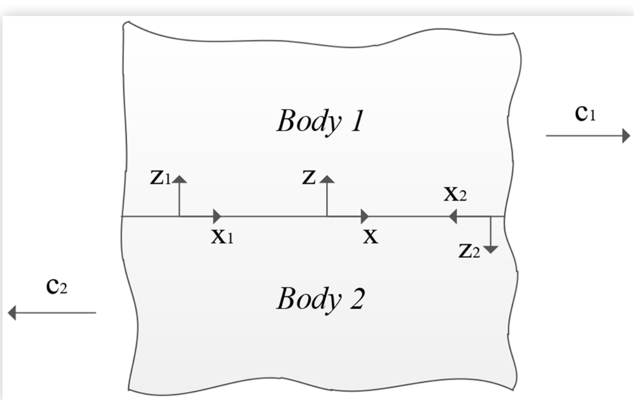

where T_j is the temperature fields of body j, k_j is the diffusivity of body j, t is the time. Its general solution is in the form as

$$T_j(x_j, z_j, t) = \text{Re}\left\{\Theta_0 e^{-\lambda_j z_j} e^{bt} e^{imx}\right\} \tag{2}$$

where Θ_0 is a unique complex constant, b is the grow rate of perturbation, i is the imaginary unit, $m = \frac{2\pi}{L}$ is the wavenumber, L is the associated wavelength, and the special decay rate, λ is defined as

$$\lambda_j = \sqrt{m^2 + \frac{b}{k_j} - \frac{imc_j}{k_j}} \tag{3}$$

The sum of all three terms of displacements of two materials must be zero to ensure conforming contact:

$$\sum_{j=1}^{2}\left(u_{zj}^{el} + u_{zj}^{th} + u_{zj}^{w}\right) = 0 \tag{4}$$

where $u_{zj}^{el}(x)$ is the elastic displacement of body j, $u_{zj}^{th}(x)$ is the thermally induced displacement, and $u_{zj}^{w}(x)$ is the wear-induced displacement that can be written

$$u_{zj}^{w}(x) = \text{Re}\left\{w_j e^{bt} e^{imx}\right\} \tag{5}$$

where w_j are complex constants of body j. By expressing the displacements and the contact pressure in the perturbation form similar to Eq. (5), the following equation is obtained.

$$p_0 = \frac{\sum_{j=1}^{2}\frac{2\alpha_j(1+\nu_j)}{m+\lambda_j}}{\frac{2}{mE^*} + V\sum_{j=1}^{2}\frac{W_j}{b - imc_j}}\Theta_0 \tag{6}$$

where p_0 is the amplitude of pressure perturbation in the expression $p(x) = p_0$ Re $\{e^{bt}e^{imx}\}$; W_j is the wear coefficient of body j; α_j is the coefficient of thermal expansion of body j; E^* is the combined elastic modulus for plane strain defined as

$$\frac{1}{E^*} = \frac{1-\nu_1^2}{E_1} + \frac{1-\nu_2^2}{E_2} \tag{7}$$

where E_1, E_2 are Young's elastic moduli of the two materials; ν_1, ν_2 are Poisson's ratios.

The total heat flux across the sliding interface is

$$q(x) = -K_1\frac{\partial T_1}{\partial z_1} - K_2\frac{\partial T_2}{\partial z_2} = \text{Re}\left\{\Theta_0\sum_{j=1}^{2}K_j\lambda_j e^{bt}e^{imx}\right\} \tag{8}$$

where K_1, K_2 are the conductivities.

Using the frictional heating equation

$$q(x) = fVp(x) \tag{9}$$

imposing Eqs. (6) ands (8), canceling out the exponents form, and defining the following dimensionless quantities:

$$\tilde{c}_j = \frac{c_j}{mk_2},\quad \tilde{\lambda}_j = \frac{\lambda_j}{m},\quad \tilde{b} = \frac{b}{m^2k_2}$$
$$\tilde{W}_1 = E^*W_1, \tilde{R}_W = \frac{W_2}{W_1}, \tilde{K}_1 = \frac{K_1}{K_2}, \tilde{k}_1 = \frac{k_1}{k_2} \tag{10}$$
$$\tilde{H}_2 = \frac{k_2 f}{K_2}E^*\alpha_2(1+\nu_2), \tilde{\alpha}_1 = \frac{\alpha_1(1+\nu_1)}{\alpha_2(1+\nu_2)}$$

the characteristic equation can finally be written in the form:

$$\left(\tilde{K}_1\tilde{\lambda}_1+\tilde{\lambda}_2\right)\left[1+i\frac{\tilde{W}_1}{2}\left|\tilde{c}_1-\tilde{c}_2\right|\left(\frac{1}{\tilde{c}_1}+\tilde{R}_W\frac{1}{\tilde{c}_2}\right)\right] \\ -\tilde{H}_2\left|\tilde{c}_1-\tilde{c}_2\right|\left(\frac{\tilde{\alpha}_1}{1+\tilde{\lambda}_1}+\frac{1}{1+\tilde{\lambda}_2}\right)=0 \quad (11)$$

1.2 Limiting Cases

1.2.1. A Conductor Sliding against a Nonconductor. The solution for the limiting case when one of the materials is a thermal non-conductor, i.e. $\tilde{K}_1=\tilde{k}_1\to 0$, was sought. In this case, the migration speed of perturbation with respect to material 1 becomes zero, therefore $c_2\to 0$, and $c_1\to V$. If $V\gg 1$, $\tilde{b}=0$ and setting

$$\tilde{\lambda}_1=\sqrt{1-i\frac{\tilde{c}_1}{\tilde{k}_j}}=\tilde{x}_1-i\tilde{y}_2,\tilde{\lambda}_2=\sqrt{1-i\tilde{c}_2}=\tilde{x}_2+i\tilde{y}_2 \quad (12)$$

we obtain

$$\tilde{x}_1=\tilde{y}_1\to\sqrt{\frac{\tilde{c}_1}{2\tilde{k}_1}},\tilde{x}_2\to 1+\frac{1}{8}\tilde{c}_2^2,\tilde{y}_2\to-\frac{\tilde{c}_2}{2}$$

Hence, Eq. (11) becomes

$$1+\frac{1}{8}\tilde{c}_2^2+\frac{1}{4}\tilde{W}_1\left(\tilde{c}_2+\tilde{R}_w\tilde{c}_1\right)-\tilde{H}_2\tilde{c}_1\left(\tilde{\alpha}_1\sqrt{\frac{\tilde{k}_1}{2\tilde{c}_1}}+\frac{1}{2}\right)=0 \quad (13)$$

and

$$1+\frac{1}{4}\tilde{W}_1\tilde{R}_w\tilde{c}_1-\frac{1}{2}\tilde{H}_2\tilde{c}_1=0 \quad (14)$$

This results in

$$\tilde{V}_{cr}=\tilde{c}_1=\frac{4}{2\tilde{H}_2-\tilde{W}_1\tilde{R}_w} \quad (15)$$

In the absence of wear, we obtain the solution for the critical speed

$$\tilde{V}_{cr}^*=\frac{2}{\tilde{H}_2}$$

If we define a special dimensionless value of wear coefficient as

$$\tilde{W}^*=\frac{2k_2fE^*\alpha_2\left(1+\nu_2\right)}{K_2}=2\tilde{H}_2$$

Eq. (15) will become $\tilde{V}_{cr}=\dfrac{2}{\tilde{H}_2\left(1-\dfrac{\tilde{W}_1}{\tilde{W}^*}\tilde{R}_w\right)}$.

Evidently, $\tilde{V}_{cr}\to\infty$ when $\tilde{W}_2=\tilde{W}^*=2\tilde{H}_2$. This means that there is a wear coefficient of the conducting material above which TEI is completely suppressed, and this is similar to what Papangelo and Ciavarella recently discovered for a slightly different geometry [5]. Notice however that if $\tilde{H}_2$ is very high, the standard "Burton" critical speed (without wear) is very low, the system is highly unstable, and the wear coefficient to make it stable is very high. On the other hand, if $\tilde{H}_2$ is very low, then the critical wear coefficient enters a practical range, but probably the system was stable already without wear, as Burton's critical speed is already high. Intermediate cases are therefore the most interesting.

1.2.2 Identical Materials. In the special case where two bodies have the identical materials (which means they also have identical wear rate), it requires $c_1=-c_2=\frac{V}{2}$. Also, Eq. (11) becomes

$$\tilde{\lambda}_1+\tilde{\lambda}_2=\tilde{H}_2\tilde{V}\left(\frac{1}{1+\tilde{\lambda}_1}+\frac{1}{1+\tilde{\lambda}_2}\right) \quad (16)$$

where $\tilde{\lambda}_1=\sqrt{1-i\frac{\tilde{V}}{2}}=x-iy$, $\tilde{\lambda}_2=\sqrt{1+i\frac{\tilde{V}}{2}}=x+iy$.

Hence Eq. (16) becomes $2\tilde{H}_2=\dfrac{x}{y}=\sqrt{\dfrac{\sqrt{1+\left(\frac{\tilde{V}}{2}\right)^2}+1}{\sqrt{1+\left(\frac{\tilde{V}}{2}\right)^2}-1}}$ along with

$$\tilde{V}=\left|\frac{8\tilde{H}_2}{4\tilde{H}_2^{\,2}-1}\right| \quad (17)$$

2. Finite Element Method

Considering a two-dimensional sliding system in which a moving body slides in the positive x-direction at constant speed V on a stationary body and makes contact over a common interface (Fig. 1), we assume that all boundaries are thermally insulated except the sliding interface. The bodies are assumed to be of infinite extent in the horizontal x-direction.

The heat conduction equation is

$$k\nabla^2T-\left(\frac{\partial T}{\partial t}+V\frac{\partial T}{\partial x}\right)=0 \quad (18)$$

where k is the thermal diffusivity. If we assume a perturbation of temperature as

$$T\left(x,y,t\right)=e^{bt+imx}\Theta\left(y\right) \quad (19)$$

where b is an exponential growth rate and m is a wavenumber. Substituting Eq. (19) into Eq. (18) yields

$$k\frac{\partial^2\Theta}{\partial z^2}-\left[km^2+\left(imV+b\right)\right]\Theta=0 \quad (20)$$

Using appropriate boundary conditions, a finite element formulation of the problem [14] can be obtained as

$$\left(\mathbf{K}+V\mathbf{C}+b\mathbf{H}\right)\Theta+Q=0 \quad (21)$$

where **K**, **C**, **H** indicate matrices and V, Θ represent vectors. Due to the results of frictional heating at the contact interface, the nodal heat sources Q is given by

$$Q=\phi fVP \quad (22)$$

where ϕ represents a coefficient matrix.

This leads to

$$\left(K^* + b\mathrm{H}\right)\Theta + \phi f V P = 0 \tag{23}$$

where

$$K^* = K + VC \tag{24}$$

where P is the corresponding vector of nodal contact forces normal to the contact interface and f is the coefficient of friction.

For the thermoelastic contact problem without considering the wear effect, a quasi-static thermoelastic equations has no time-dependent terms and has also no dependence on the velocity V or the growth rate b. Thus, the contact forces are coupled with the temperature and displacement field as

$$\begin{bmatrix} L_1 \\ L_2 \end{bmatrix} U - \begin{bmatrix} G_1 \\ G_2 \end{bmatrix} \Theta = MP \tag{25}$$

where **M** is a coefficient matrix.

If we consider the wear effect prescribed by the Archard law, i.e. $\dot{\delta} = WVP$ where W is the wear coefficient, and the conforming contact condition expressed in such a way that the deformation of the moving body is equal to the thermal expansion subtracted by the amount of wear. For simplicity we assume wear takes place on material 1 only, and the technique will later be extended to include wear on both materials. To do this we partition $\mathbf{L}_1$ into $\mathbf{L}_{11}$ and $\mathbf{L}_{12}$ to separate the portion in $\mathbf{L}_1$ associated with the z-displacement of the contacting nodes in material 1, namely U_1 from the rest degrees of freedom of the system, namely U_2. The wear condition modifies the contact boundary condition of Eq. (25) as

$$\begin{bmatrix} \mathrm{L}_{11} & \mathrm{L}_{12} \\ \mathrm{L}_{21} & \mathrm{L}_{22} \end{bmatrix} \begin{bmatrix} U_1 - \int WVPdt \\ U_2 \end{bmatrix} - \begin{bmatrix} \mathrm{G}_1 \\ \mathrm{G}_2 \end{bmatrix} \Theta = \mathrm{M}P \tag{26}$$

where **M** is a constant matrix. The wear problem is dependent on time and the growth rate b. Thus, if the displacement, contact pressure, and temperature are expressed as Ue^{bt}, Pe^{bt}, Θe^{bt} and Eq. (26) is differentiated with respect to t, we can obtain

$$\begin{bmatrix} \mathrm{L}_{11} & \mathrm{L}_{12} \\ \mathrm{L}_{21} & \mathrm{L}_{22} \end{bmatrix} \begin{bmatrix} bU_1 - WVP \\ bU_2 \end{bmatrix} - \begin{bmatrix} \mathrm{G}_1 \\ \mathrm{G}_2 \end{bmatrix} \Theta = \mathrm{M}P \tag{27}$$

Considering that the tractions exerted on the contacting surface pairs have opposite signs, we may rearrange this equation to obtain

$$\begin{cases} b\mathrm{L}_1 U - \mathrm{L}_{11} WVP - b\mathrm{G}_1 \Theta = 0 \\ b\mathrm{L}_2 U - \mathrm{L}_{21} WVP - b\mathrm{G}_2 \Theta = 0 \end{cases} \tag{28}$$

In deriving this equation, we combined some equations together to make the right hand side of the equations to be zero. This is possible because the tractions cancel out at the contacting nodes by addition and the external loading is zero at the interior nodes. Combining the two equations by eliminating U leads to

$$\mathrm{L}^* VP + b\mathrm{G}^* \Theta - bP = 0 \tag{29}$$

where

$$\mathrm{L}^* = W\left(\mathrm{L}_0 \mathrm{L}_2^{-1} \mathrm{L}_{21} - \mathrm{L}_{01}\right) \tag{30}$$

and

$$\mathrm{G}^* = \mathrm{L}_0 \mathrm{L}_2^{-1} \mathrm{G}_2 - \mathrm{G}_0 \tag{31}$$

Putting together Eqs (23), and (29) yields

$$\left(\begin{bmatrix} \mathrm{L}^* V & \mathrm{O} \\ \phi f V & \mathrm{K}^* \end{bmatrix} - b \begin{bmatrix} \mathrm{I} & -\mathrm{G}^* \\ \mathrm{O} & -\mathrm{H} \end{bmatrix} \right) \tilde{X} = 0 \tag{32}$$

where

$$\tilde{X} = \begin{Bmatrix} P \\ \Theta \end{Bmatrix} \tag{33}$$

This is a standard eigenvalue problem, in which the growth rate b is the eigenvalue. However, we encountered numerical difficulties in directly solving this equation sometimes. We instead converted this equation into a higher order eigenvalue problem by eliminating the degrees of freedom associated with the pressure, P in $\tilde{X}$. The final result becomes

$$b^2 \mathrm{A}_2 \Theta + b\mathrm{A}_1 \Theta - \mathrm{A}_2 \Theta = 0 \tag{34}$$

in which

$$\mathrm{A}_0 = -\mathrm{L}^* V \mathrm{K}^* \tag{35}$$

$$\mathrm{A}_1 = \mathrm{K}^* - \mathrm{H}\mathrm{Q}^* V - \phi f V \mathrm{G}^* \tag{36}$$

$$\mathrm{A}_2 = \mathrm{H} \tag{37}$$

This is a second-order polynomial eigenvalue equation, for which the solution method is well known. Namely, we convert Eq. (34) into two first order eigenvalue equations

$$\left(\begin{bmatrix} \mathrm{A}_0 & \mathrm{A}_1 \\ \mathrm{O} & \mathrm{I} \end{bmatrix} - b \begin{bmatrix} \mathrm{O} & -\mathrm{A}_2 \\ \mathrm{I} & \mathrm{O} \end{bmatrix} \right) \begin{Bmatrix} \Theta \\ \tilde{\Theta} \end{Bmatrix} = 0 \tag{38}$$

and

$$\tilde{\Theta} = b\Theta \tag{39}$$

It was found that the solutions from Eqs. (38) and (39) converged much better than Eq. (32). The above discussion is based on the assumption that wear is absent in material 2. To incorporate the effect of wear from both materials, all equations remain the same except that $\mathbf{L}^*$ has to be redefined as

$$\mathrm{L}^* = \mathrm{L}_0 \mathrm{L}_2^{-1} \left(\mathrm{L}_{21a} W_a + \mathrm{L}_{21b} W_b \right) - \left(\mathrm{L}_{01a} W_a + \mathrm{L}_{01b} W_b \right) \tag{40}$$

where the subscript a and b are used to indicate the two different materials.

Results and Discussions

In order to validate the results from the finite element analysis (FEA), we referred to Papangelo and Ciavarella[6] but assume that $\tilde{H}_2 = 0.0013$, $\tilde{\alpha}_1 = 2.5$, $\tilde{K}_1 = \tilde{k}_1$. We assumed $\tilde{H}_2 = 0.0013$ rather than 0.34 here because we intended to fix a misprint in [6]. We first compared the three solutions: Burton's analytic solution [2], Papangelo and Ciavarella's solution and FEA solution in the limiting case when there is no wear. As is shown in the Fig. 2, all solutions for $\tilde{W}_1 / \tilde{W}^* = 0$ vary linearly with respect to the thermal conductivity. In Fig. 2(a), when Poisson's

FIGURE 2 The comparison of solutions of Burton, Papangelo and FEA as a function of the conductivity $\tilde{K}_1 = \tilde{k}_1$ for wear rate $\tilde{W}_1/\tilde{W}^* = 0$, $\tilde{H}_2 = 0.0013$, $\tilde{\alpha}_1 = 2.5$, different values of ν=0(a) or 0.3(b).

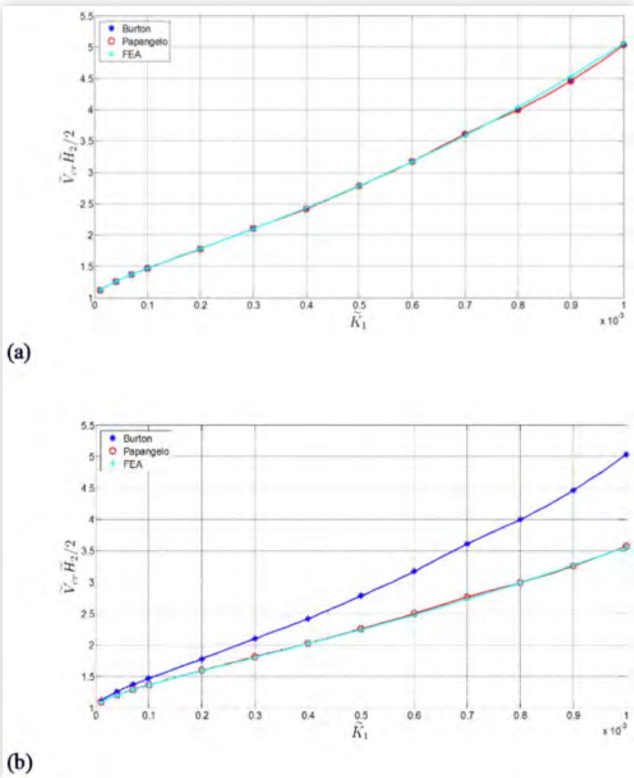

FIGURE 3 The comparison of solutions of analytic and FEA as a function of the conductivity $\tilde{K}_1\left(=\tilde{k}_1\right)$ for $\tilde{H}_2 = 0.34$, $\tilde{\alpha}_1 = 2.5$, $\tilde{R}_w = 0.1$ different values of wear rate $\tilde{W}_1/\tilde{W}^* = [0.1,0.4,0.7,1]$.

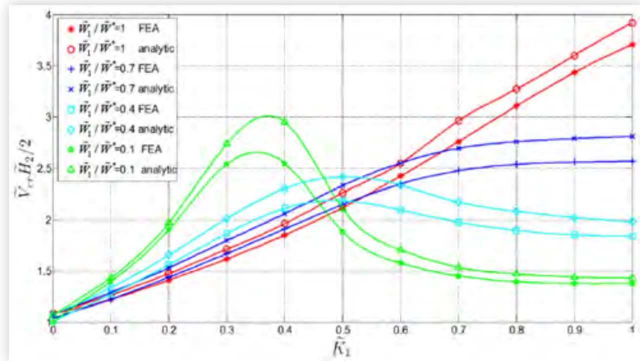

FIGURE 4 The comparison of solutions of analytic and FEA as a function of the conductivity $\tilde{K}_1\left(=\tilde{k}_1\right)$ for $\tilde{H}_2 = 0.34$, $\tilde{\alpha}_1 = 2.5$, $\tilde{R}_w = 0$, different values of wear rate $\tilde{W}_1/\tilde{W}^* = [0,0.1]$.

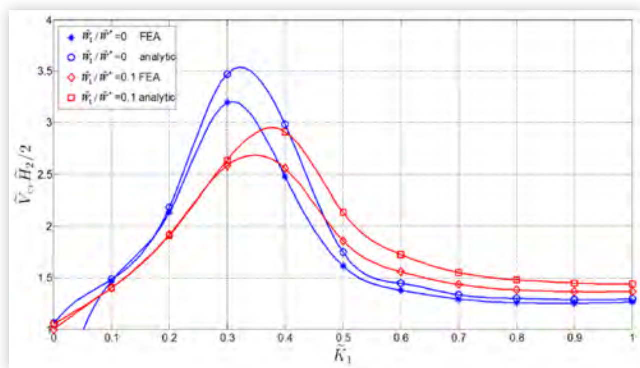

ratio ν is set to zero, solutions of Burton, Papangelo and FEA are nearly identical. When Poisson's ratio is greater than 0 (ν=0.3) as shown in Fig. 2(b), he solutions from Papangelo and FEA are comparable, but different from Burton's. This is because the effect of Poisson's ratio is neglected in Burton's solution, while Papangelo and FEA took the plane strain equality by considering the effect of Poisson's ratio. Since the FEA solution agrees with Papangelo's solution much better than Burton's, we decided to use Papangelo's analytic solutions to validate the FEA results in the following discussions.

Practically the wear rate is not zero and two materials have different wear rates. We first assume $\tilde{R}_w = 0.1$, i.e. material 2 has a wear rate 10% of that of material 1. Fig. 3 shows the comparison between the analytic and FEA solutions as a function of the conductivity $\tilde{K}_1\left(=\tilde{k}_1\right)$ for $\tilde{H}_2 = 0.34$, $\tilde{\alpha}_1 = 2.5$, with different values of wear rate $\tilde{W}_1/\tilde{W}^* = [0.1,0.4,0.7,1]$. We assumed $\tilde{H}_2 = 0.34$ here because it is easier to compare the FEA solution to analytical solution in [6]. This value has been used in the current study to maintain consistency. As is shown above, the analytic and FEA solutions exhibit the same trend of variation. When $\tilde{W}_1/\tilde{W}^*$ = 0.1 or 0.4, the FEA and analytic solutions increase at the beginning before they decrease. When $\tilde{W}_1/\tilde{W}^*$ = 0.7 or 1, the solutions of FEA and analytic are monotonic with $\tilde{K}_1$. The difference between the two solutions also gradually increases with $\tilde{K}_1$, with a maximum value around 14%. It has also been found that the maximum difference between the two solutions decreases with the wear rate. When the dimensionless wear rate $\tilde{W}_1/\tilde{W}^*$ is set to 1, the maximum difference is 5.47%. When $0.1 < \tilde{K}_1 < 0.5$, the critical speed *decreases* as $\tilde{W}_1/\tilde{W}^*$ increases, therefore wear *destabilizes* the system; On the other hand, when $\tilde{K}_1 > 0.5$, the critical speed increases with $\tilde{W}_1/\tilde{W}^*$, therefore wear stabilizes the system by suppressing TEI. When $\tilde{K}_1 \to 0$, the result is complex because of the computational accuracy.

We investigated the special case where material 2 does not involve wear, i.e. $\tilde{R}_w = 0$. Fig. 4 shows the comparison of the analytic and FEA solutions as a function of the conductivity $\tilde{K}_1\left(=\tilde{k}_1\right)$ for $\tilde{H}_2 = 0.34$, $\tilde{\alpha}_1 = 2.5$, $\tilde{R}_w = 0$, and different values of wear rate $\tilde{W}_1/\tilde{W}^* = [0,0.1]$. There are a number of similarities between the analytic and FEA solutions. It reveals that there is a steep rise when $\tilde{K}_1$ ″ 0.3 for $\tilde{W}_1/\tilde{W}^* = 0$, then it gradually drops. As for $\tilde{W}_1/\tilde{W}^* = 0.1$, the variation trend is the same, but the curve is flattened. The maximum difference between the two solutions is by around 16%. The transition of the effect on TEI occurs at $\tilde{K}_1 = 0.4$: When $0.1 < \tilde{K}_1 < 0.4$, TEI is amplified; Otherwise, TEI is suppressed.

In addition, the results are presented as a function of the wear rate by assuming $\tilde{H}_2 = 0.34$, $\tilde{\alpha}_1 = 2.5$, $\tilde{K}_1 = \tilde{k}_1$, $\tilde{R}_w = 0.1$ in Fig. 5. Clearly the analytical and FEA solutions as a function of the wear rate $\tilde{W}_1/\tilde{W}^*$ for $\tilde{K}_1 = [0.01,0.1,0.5,1]$ tend to vary in the same pattern. The critical speed is quite stable with the wear rate $\tilde{W}_1/\tilde{W}^*$ when the conductivity $\tilde{K}_1$ is less than 0.5. It

FIGURE 5 The comparison of solutions of analytic and FEA as a function of the wear rate $\tilde{W}_1 / \tilde{W}^*$ for $\tilde{H}_2 = 0.34$, $\tilde{\alpha}_1 = 2.5$, $\tilde{K}_1 = \tilde{k}_1$, different values of conductivity $\tilde{K}_1 = \lceil 0.01, 0.1, 0.5, 1 \rceil$.

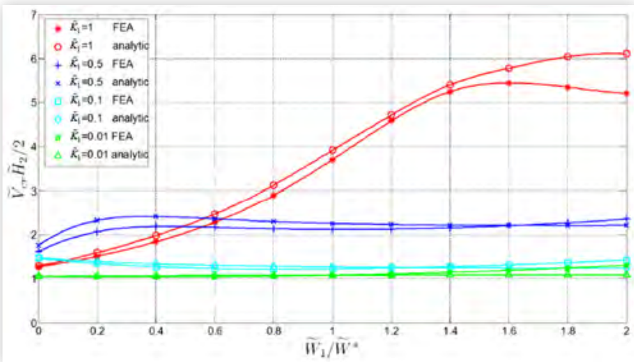

FIGURE 6 Comparison of analytic and FEA solutions as a function of the wear rate $\tilde{W}_1 / \tilde{W}^*$ for $\tilde{R}_w = 0.3$, $\tilde{K}_1 = 0.01$, $\tilde{H}_2 = 0.34$, $\tilde{\alpha}_1 = 2.5$, $\tilde{K}_1 = \tilde{k}_1$.

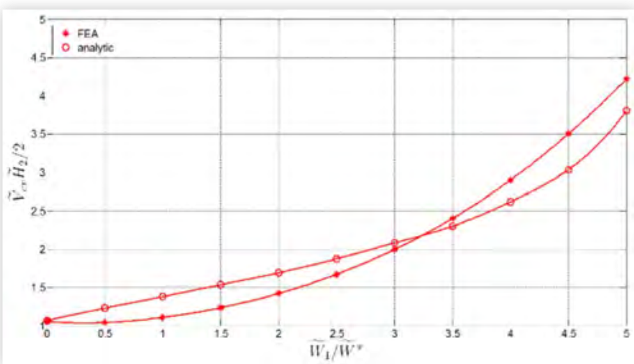

can be seen in this figure that the critical speed steadily increases when $\tilde{K}_1 = 1$ and $\tilde{W}_1 / \tilde{W}^* < 1.6$. When the wear rate $\tilde{W}_1$ is greater than the critical wear rate $\tilde{W}^*$, the discrepancy between the two solutions could become significant. For example, the two solutions deviate from each other by no more than 11.1% when $\tilde{W}_1 / \tilde{W}^* < 1$. However, when $\tilde{W}_1 / \tilde{W}^* = 2$ and $\tilde{K}_1 = 1$, the difference becomes as large as 15%.

We also investigated the case where the ratio of the two wear rates $\tilde{R}_w$ is greater than 0.1. Fig. 6 shows the comparison of the analytic and FEA solutions as a function of the wear rate $\tilde{W}_1 / \tilde{W}^*$ for $\tilde{R}_w = 0.3, \tilde{K}_1 = 0.01, \tilde{H}_2 = 0.34, \tilde{\alpha}_1 = 2.5, \tilde{K}_1 = \tilde{k}_1$. The two solutions are close to each other as $\tilde{W}_1 / \tilde{W}^*$ ranges from 0 to 5. When $\tilde{W}_1 / \tilde{W}^* \leq 3$, the analytical solution is almost linear, while the FEA solution exhibits an apparent nonlinearity. The analytical solution is greater than the finite element solution in this domain. When $\tilde{W}_1 / \tilde{W}^* > 3$, however, the analytical solution falls below the FEA solution.

These differences are largely induced by the numerical errors in the finite element approach, as well as the convergence issue in the analytical approach when the solution drastically oscillates across the thickness. Four possible sources of error have been summarized as follows:

1. The analytical solution was based on the half-space geometries. However, it is known that infinite dimensions are not allowed in the finite element model. Instead a reasonably large thickness, e.g. has been assumed in the latter to approximate half planes.
2. The finite element analysis led to a nonlinear eigenvalue equation whose solution is significantly more unstable than a linear eigenvalue problem.
3. It is known that the temperature field is highly oscillating with a substantially large gradient near the friction interface. A biased finite element mesh towards the sliding interface has thus been implemented. On the other hand, the differences in the element sizes should not be too large in a finite element model. Otherwise it may lead to a scaling problem in the matrix operations, causing a noticeable numerical inaccuracy.
4. The problem is highly nonlinear and the analytical solution itself is sometimes unstable when the parameters are chosen in a certain way. Therefore the analytical solution does not necessarily converge in this study. For example, the analytical solution starts to diverge when the wear coefficient well exceeds the critical value.

Conclusions

A finite element approach was implemented to study the effect of wear on frictionally excited thermoelastic instability. The classical theory was augmented by including the wear law. The governing equations on the contact pressure, temperature and displacement were reduced to a quadratic eigenvalue equation, where the eigenvalue is the exponential growth rate of perturbation and the eigenvector is the nodal temperature. The solution was sought via a conversion of the nonlinear problem into two ordinary linear eigenvalue equations. The computational results based on a simplified, two-dimensional model generally show good agreements with those of the analytical solution assuming an infinite thickness and conforming contact. However, the noticeable differences exist between the two approaches in some situations when the numerical instability starts to dominate due to the high nonlinearity in the solutions.

The conclusions from the analytical approach has been confirmed that depending on the chosen parameters wear may suppress or amplify TEI induced hot spotting. The advantage of the finite element method lies in the fact that there is no restriction on the geometric complexities and boundary conditions. Further studies are needed in the future, especially on the role of wear in more realistic, three-dimensional geometries such as automotive brake and clutch discs.

References

1. Barber, J.R., "Thermoelastic Instabilities in the Sliding of Conforming Solids," *Proceedings of the Royal Society of London A* 312:381-394, 1969.

2. Burton, R.A., Nerlikar, V., and Kilaparti, S.R., "Thermoelastic Instability in a Seal-Like Configuration," *Wear* 24:177-188, 1973.
3. Dow, T.A., and Burton, R.A., "Thermoelastic Instability of Sliding Contact in the Absence of Wear," *Wear* 19:315-328, 1972.
4. Dow, T.A., and Burton, R.A., "The Role of Wear in the Initiation of Thermoelastic Instabilities of Rubbing Contact," *Journal of Lubrication Technology* 95:71-75, 1973.
5. Papangelo, A., and Ciavarella, M., "Can Wear Completely Suppress Thermoelastic Instabilities?" *Journal of Tribology* 142:3-8, 2020.
6. Papangelo, A., and Ciavarella, M., "The Effect of Wear on ThermoElastic Instabilities (TEI) in Biomaterial Interfaces," *Tribology International* 142:1-6, 2020.
7. Ciavarella, M., Decuzzi, P., and Monno, G., "Frictionally-Excited Thermoelastic Contact of Rough Surfaces," *International Journal of Mechanical Sciences* 42:1307-1325, 2000.
8. Decuzzi, P., Ciavarella, M., and Monno, G., "Frictionally Excited Thermoelastic Instability in Multi-disk Clutches and Brakes," *Journal of Tribology* 123:865-871, 2001.
9. Lee, K., and Barber, J.R., "Frictionally Excited Thermoelastic Instability in Automotive Disk Brakes," *Journal of Tribology* 115:607-614, 1993.
10. Hartsock, D.L., and Fash, J.W., "Effect of Pad/Caliper Stiffness, Pad Thickness, and Pad Length on Thermoelastic Instability in Disk Brakes," *Journal of Tribology* 122:511-518, 2000.
11. Abbasi, S., Teimourimanesh, S., and Vernersson, T., "Temperature and Thermoelastic Instability at Tread Braking Using Cast Iron Friction Material," *Wear* 314:171-180, 2014.
12. Wang, Q.L., Cui, H.W., Lian, Z.S., and Li, L., "Thermoelastic Analysis of Friction Pairs in Hydro-Viscous Drive Combined Thermal and Mechanical Loads under Soft Startup Condition," *Numerical Heat Transfer, Part A: Applications* 75:327-341, 2019.
13. Chen, Z., Yi, Y.B., Bao, K., and Zhao, J.X., "Numerical Analysis of the Coupling between Frictionally Excited Thermoelastic Instability and Thermal Buckling in Automotive Clutches," *Proc IMechE Part J: J Engineering Tribology* 0:1-10, 2018.
14. Yi, Y.B., "Finite Element Analysis of Thermoelastodynamic Instability Involving Frictional Heating," *Journal of Tribology* 128:718-724, 2006.
15. Yi, Y.B., Bendawi, A., Li, H.Y., and Zhao, J.X., "Finite Element Analysis of Thermoelastic Instability in Intermittent Sliding Contact," *Journal of Thermal Stresses* 37:870-883, 2014.
16. Liu, Y.W., Jang, Y.H., and Barber, J.R., "Finite Element Implementation of an Eigenfunction Solution for the Contact Pressure Variation due to Wear," *Wear* 309:134-138, 2014.
17. Belhocine, A., and Abdullah, O.I., "A Thermomechanical Model for the Analysis of Disc Brake Using the Finite Element Method in Frictional Contact," *Journal of Thermal Stresses* 43:305-320, 2019.
18. Zhao, J.X., *Research on Thermoelastic Instability of Shifting Clutches in the Process of Engagement* (Beijing: Beijing Institute of Technology, 2014).
19. Zhao, J.X., Chen, Z., Yang, H.Z., and Yi, Y.B., "Finite Element Analysis of Thermal Buckling in Automotive Clutch Plates," *Journal of Thermal Stresses* 39:77-89, 2016.
20. Graf, M., and Ostermeyer, G.P., "Efficient Computation of Thermoelastic Instabilities in the Presence of Wear," *Wear* 312:11-20, 2014.
21. Abdullah, O.I., Akhtar, M.J., and Schlattmann, J., "Investigation of Thermo-Elastic Behavior of Multidisk Clutches," *Journal of Tribology ASME* 137:1-9, 2015.

Contact Information

Yun-Bo Yi, Ph.D.
Professor
Mechanical & Materials Engineering
University of Denver
2155 E Wesley Ave
Denver, CO 80208
Yun-Bo.Yi@du.edu
Phone: 303-871-2228

ISSN 0148-7191